한국도로학회 논문집
第7券4號 2005年 12月
pp. 141 ~ 150

지반위에 놓인 콘크리트 슬래브의 수직하중에 대한 슬래브 하부의 수평 저항의 영향 분석

Effect of Horizontal Resistance at Slab Bottom on Behavior of Concrete Slabs-on-Grade under Vertical Loads

심 재 수* 김 성 민**
Shim, Jae Soo Kim, Seong Min

Abstract

The behavior of the concrete slabs-on-grade considering the horizontal resistance at the slab bottom, which exists due to the shear resistance of the foundation and the friction between the slab and the foundation, has been investigated when the slabs-on-grade are subjected to the vertical load. Analytical formulations have been developed to include the effect of the horizontal resistance at the slab bottom, and the solutions have been obtained in the transformed field domain using the Fourier transform. Finite element formulations have also been developed using the plate bending elements and the flat shell elements. The solutions from the analytical and numerical models have been compared and showed very good agreement. The sensitivity of the horizontal resistance to the stresses of the concrete slab has been investigated with various values of the slab thickness, elastic modulus, and vertical stiffness of the foundation. The analysis results show that the horizontal resistance at the plate bottom can significantly affect the stresses of the slab.

Keywords : concrete, slab-on-grade, horizontal resistance, vertical load, finite element, fourier transform, transformed field

요 지

지반위에 놓인 콘크리트 슬래브가 수직하중을 받을 때 지반의 전단저항과 슬래브 하부와 지반과의 마찰 등에 의해 생기는 슬래브 하부의 수평저항을 고려하여 지반위에 놓인 콘크리트 슬래브의 거동을 분석하였다. 슬래브 하부의 수평저항을 고려하기 위한 해석 공식을 유도하였고 퓨리에변환을 이용한 변환영역에서 이러한 공식의 해를 구하였다. 또한 판요소와 쉘요소를 이용한 유한요소법에 의한 모델을 개발하여 수치해석 결과도 도출하였다. 이러한 해석 공식과 수치해석 모델을 이용한 해석 결과를 비교 분석하였고 매우 비슷한 결과가 도출되는 것을 알 수 있었다. 콘크리트 슬래브의 응력 분포에 슬래브 하부의 수평저항이 미치는 민감성을 여러 가지의 다른 슬래브의 두께, 탄성계수, 그리고 지반의 수직탄성계수 등을 고려하여 분석하였다. 해석 결과에서 슬래브 하부의 수평저항은 슬래브의 응력에 매우 큰 영향을 미칠 수 있다는 것을 발견하였다.

핵심용어 : 콘크리트, 지반위의 슬래브, 수평저항, 수직하중, 유한요소, 퓨리에변환, 변환영역

* 정회원 · 경희대학교 토목건축대학 교수 · 공학박사
** 정회원 · 경희대학교 토목건축대학 조교수 · 공학박사 · 교신저자

1. Introduction

A number of studies have been performed to analyze the behavior of Portland cement concrete (PCC) slabs-on-grade including PCC pavement systems analytically and numerically by employing the plate on an elastic foundation (Westergaard, 1925; Tabatabaie and Barenberg, 1980; Huang, 1993; Kim and Roesset, 1997; Liu et al., 2000; Kim et al., 2002). The PCC slab is analyzed based on the Kirchhoff thin plate theory and the underlying layers are modeled using an elastic foundation, normally a Winkler type foundation. Accordingly, the resistance considered at the slab bottom is the vertical stiffness of the foundation (modulus of subgrade reaction) and the horizontal resistance at the slab bottom is normally ignored (Kim and Roesset, 1998; Huang and Thambiratnam, 2001). However, the shear resistance of the foundation and the friction between the slab bottom and the foundation cause the horizontal resistance applied to the bottom of the slab. If the slab and the foundation are perfectly bonded, the horizontal resistance at the slab bottom will be the same as the shear resistance of the foundation. Even if the slab and the foundation are perfectly debonded, the interface friction will still cause the horizontal resistance at the slab bottom. The horizontal resistance exerts its effect when there are horizontal strains at the slab bottom, which is common with most types of the loads including vertical load, moment, surface traction, temperature gradient, and temperature drop and increase.

The horizontal resistance at the slab bottom can simply be considered by attaching horizontal springs at the slab bottom when the slab is modeled using three-dimensional (3D) solid finite elements (Kim et al., 2000). However, computation run time and needed memory to obtain the analysis results are significantly larger for the 3D analysis than those for the analysis based on the plate theory. When the plate on an elastic foundation is analyzed using the plate bending or shell finite elements, the horizontal resistance at the plate bottom cannot be considered directly by attaching the horizontal springs to the degrees of freedom of the finite elements because the degrees of freedom considered in the plate bending or shell elements are assumed to exist at the middle surface of the plate.

In this paper, the methods to include the horizontal resistance at the slab bottom are presented when considering the thin plate theory. In the first part of the paper, the analytical formulations are derived first and the numerical formulations to include the horizontal resistance at the slab bottom are explained when using the plate bending finite elements. The analytical and numerical analysis results are compared and the effects of the horizontal resistance on the stresses are investigated when the PCC slabs-on-grade are subjected to a vertical load. In the second part of the paper, the numerical formulations to include the horizontal resistance at the slab bottom are presented when using the shell elements containing five degrees of freedom at each finite element node. Then, the analysis results are compared with those from a more rigorous 3D model. The effects of the horizontal resistance at the slab bottom are investigated when the system is subjected to a vertical load. Finally, the findings from this study are summarized.

2. Formulations including horizontal resistance at slab bottom

2.1. Analytical formulations

If a plate on a Winkler foundation has horizontal resistance at the bottom of the plate, as shown in Fig. 1, the horizontal resistance will cause internal horizontal forces to the plate bottom when the plate is subjected to

external loads. In a Cartesian coordinate system {*x, y, z*}, if a horizontal force at the plate bottom in the x direction per unit length in the *y* direction is *f(x, y)*, the variation of the horizontal force in the *x* direction in a small segment d_x of the plate is

$$\frac{\partial f(x,y)}{\partial x}dx \tag{1}$$

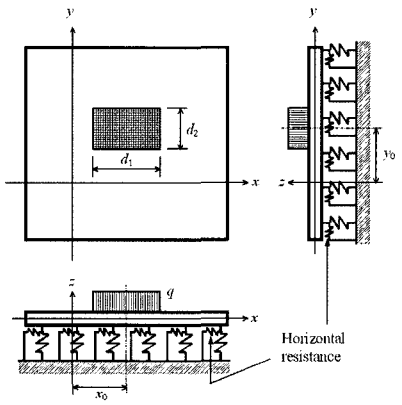

Fig. 1. Plate on Winkler foundation with horizontal resistance at plate bottom

This horizontal force variation at the plate bottom causes a bending moment with respect to the middle (neutral) surface of the plate and the moment can be calculated by

$$\frac{\partial f(x,y)}{\partial x}dx\frac{h}{2} \tag{2}$$

where *h* is the thickness of the plate. If the Kirchhoff thin plate theory is considered, equilibrium of the moments around the *y* axis can be obtained by

$$\frac{\partial m_x(x,y)}{\partial x}+\frac{\partial m_{yx}(x,y)}{\partial y}-\frac{\partial f(x,y)}{\partial x}\frac{h}{2}=s_x(x,y) \tag{3}$$

where $m_x(x, y)$ and $m_{yx}(x, y)$ are the bending and twisting moments, respectively, per unit length around the *y* axis, and $s_x(x, y)$ is the transverse shear force per unit length in the *x* direction. If the horizontal resistance (stiffness per unit area) at the plate bottom is k_h, the force differential $\partial f(x,y) / \partial x$ can be rewritten as

$$\frac{\partial f(x,y)}{\partial x}=-k_h\frac{h}{2}\frac{\partial w(x,y)}{\partial x} \tag{4}$$

where *w(x, y)* is the vertical displacement. After considering equilibrium of the moments around the *x* axis similarly, Eq. (5) can be obtained by inserting the moment equilibrium equations into the equilibrium equation of the forces in the *z* direction.

$$\frac{\partial^2 m_y(x,y)}{\partial x^2}+2\frac{\partial^2 m_{yx}(x,y)}{\partial x\,\partial y}+\frac{\partial^2 m_x(x,y)}{\partial y^2}+\frac{h^2k_h}{4}\left(\frac{\partial^2 w(x,y)}{\partial x^2}+\frac{\partial^2 w(x,y)}{\partial y^2}\right)-kw_v(x,y)=-q(x,y) \tag{5}$$

where $m_y(x, y)$ is the bending moment per unit length around the x axis; $m_{yx}(x, y)$ is the twisting moment per unit length around the *x* axis, which is the same as $m_{xy}(x, y)$; k_v is the vertical stiffness of the foundation per unit area; and *q(x, y)* is the external vertical force per unit area. By expressing the internal moments m_x, m_y, and m_{xy}, in Eq. (5) in terms of the vertical displacement *w(x, y)*, the governing differential equation can be obtained by

$$D_P\left(\frac{\partial^4 w(x,y)}{\partial x^4}+2\frac{\partial^4 w(x,y)}{\partial x^2\partial y^2}+\frac{\partial^4 w(x,y)}{\partial y^4}\right)-\frac{h^2k_h}{4}\left(\frac{\partial^2 w(x,y)}{\partial x^2}+\frac{\partial^2 w(x,y)}{\partial y^2}\right)+k_v w(x,y)=q(x,y) \tag{6}$$

where D_P is the flexural rigidity of the plate defined by

$$D_P=\frac{Eh^3}{12(1-\nu^2)} \tag{7}$$

and *E* and *v* are the elastic modulus and Poisson' s ratio of the plate, respectively.

The solution of Eq. (6) can be obtained using the Fourier transform if the plate is assumed to extend to infinity in the horizontal plane. If ξ and ζ are assumed to be the transformed fields of *x* and *y* and if *w(x, y)* and *q(x, y)* are written in the form of $W(\xi,\zeta)e^{i\xi x}e^{i\zeta y}$ and, $Q(\xi,\zeta)e^{i\xi x}e^{i\zeta y}$ the transformed displacement W(ξ, ζ) can be obtained by

$$W(\xi,\zeta)=\frac{Q(\xi,\zeta)}{D_P(\xi^2+\zeta^2)^2+\frac{h^2k_h}{4}(\xi^2+\zeta^2)+k_v} \tag{8}$$

where the transformed load $Q(\xi, \zeta)$ is obtained using the double Fourier transform

$$Q(\xi,\zeta)=\int_{-\infty}^{\infty}\int_{-\infty}^{\infty} q(x,y)\ e^{-i\xi x}e^{-i\zeta y}\ dxdy \tag{9}$$

Then, the vertical displacements can be obtained using the double inverse Fourier transform

$$w(x,y)=\frac{1}{(2\pi)^2}\int_{-\infty}^{\infty}\int_{-\infty}^{\infty}\frac{Q(\xi,\zeta)}{D_P(\xi^2+\zeta^2)^2+\frac{h^2k_h}{4}(\xi^2+\zeta^2)+k_v}e^{i\xi x}e^{i\zeta y}d\xi d\zeta \tag{10}$$

Finally, the stresses in the x and y directions can be obtained by

$$\sigma_x(x,y,z)=-\frac{Ez}{1-\nu^2}\left(\frac{\partial^2 w}{\partial x^2}+\nu\frac{\partial^2 w}{\partial y^2}\right)$$

$$=\frac{Ez}{(1-\nu^2)(2\pi)^2}\int_{-\infty}^{\infty}\int_{-\infty}^{\infty}\frac{(\xi^2+\nu\zeta^2)Q(\xi,\zeta)}{D_P(\xi^2+\zeta^2)^2+\frac{h^2k_h}{4}(\xi^2+\zeta^2)+k_v}e^{i\xi x}e^{i\zeta y}d\xi d\zeta \tag{11}$$

$$\sigma_y(x,y,z)=-\frac{Ez}{1-\nu^2}\left(\frac{\partial^2 w}{\partial y^2}+\nu\frac{\partial^2 w}{\partial x^2}\right)$$

$$=\frac{Ez}{(1-\nu^2)(2\pi)^2}\int_{-\infty}^{\infty}\int_{-\infty}^{\infty}\frac{(\nu\xi^2+\zeta^2)Q(\xi,\zeta)}{D_P(\xi^2+\zeta^2)^2+\frac{h^2k_h}{4}(\xi^2+\zeta^2)+k_v}e^{i\xi x}e^{i\zeta y}d\xi d\zeta \tag{12}$$

In practice, the above equations are solved using the Fast Fourier Transform (FFT), which is a discrete transform.

If the model shown in Fig. 1 is used and the load pressure (load per unit area) is q, the transformed load Q defined in Eq. (9) can be obtained by

$$Q(\xi,\zeta)=4q\frac{\sin\frac{d_1\xi}{2}\sin\frac{d_2\zeta}{2}}{\xi\zeta}e^{-i\xi x_0}e^{-i\zeta y_0} \tag{13}$$

where d_1 and d_2 are the loaded lengths of a distributed load in the x and y directions, respectively, and x_0 and y_0 are the coordinates of the center of the load.

2.2. Finite element modeling

As explained with Eqs (1) through (4), the horizontal resistance at the plate bottom can be transferred to the rotational resistance at the neutral surface of the plate with the rotational stiffness per unit area of

$$\frac{h^2k_h}{4} \tag{14}$$

This rotational resistance can be modeled using rotational springs around the x and y axes. The rotational stiffness K_R at each finite element node can be obtained multiplying the rotational stiffness per unit area in Eq. (14) by the effective area around the node.

$$K_R=\frac{h^2k_h}{4}\bullet(Effective\ area) \tag{15}$$

If a 4-noded linear plate bending finite element is considered (Fig. 2), the effective area at each node is a quarter of the element area.

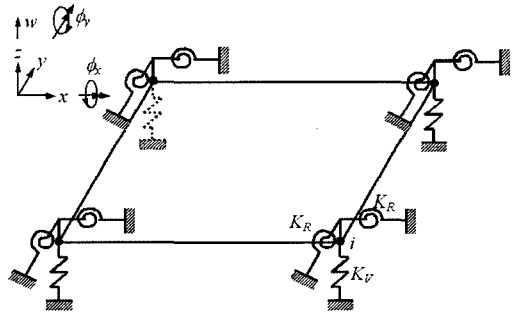

Fig. 2. Plate element with rotational springs

If the Kirchhoff thin plate theory is applied, each finite element node has three degrees of freedom, which are a displacement in the z direction and rotational displacements around the x and y axes. The equilibrium equation at finite element node i shown in Fig. 2 can then be written as

$$\{F_i\}=\left(\begin{bmatrix}Stiffness\ matrix\ of\\ plate\ bending\\ relative\ to\ node\ i\end{bmatrix}+\begin{bmatrix}K_V & 0 & 0 & 0 & \cdots & 0\\ 0 & K_R & 0 & 0 & \cdots & 0\\ 0 & 0 & K_R & 0 & \cdots & 0\end{bmatrix}\right)\begin{Bmatrix}w_i\\ \phi_{xi}\\ \phi_{yi}\\ \vdots\end{Bmatrix} \tag{16}$$

where F_i are the forces at node i, w_i is the vertical

displacement at node i, and ϕ_{xi} and ϕ_{yi} are the rotational displacements around the x and y axes, respectively, at node i. The vertical stiffness of the foundation K_v can be obtained multiplying the vertical stiffness of the foundation per unit area k_v by the effective area.

3. Effects of horizontal resistance

The effects of the horizontal resistance at the plate bottom on the stresses of the plate are investigated when the plate on a Winkler foundation is subjected to a vertical distributed load. The properties of the plate on a Winkler foundation and the applied load used in this study are listed in Table 1.

Table 1. Properties of the plate on a Winkler foundation and applied loads

Plate Properties	
E	27,560Mpa(4,000ksi)
v	0.15
k_v	108.8 MN/m^3(400pci)
h	304.8mm(12in)
Thermal expansion coefficient	0.0000108/℃(0.000006/°F)
Load Properties	
Total load	-44.4kN(-10kip)
d_1 and d_2	304.8mm(12in.)

3.1. Comparison between analytical and numerical analysis results

The stresses at the bottom of the plate predicted by the analytical and finite element methods are compared first when a distributed load is applied on an infinitely large plate on a Winkler foundation. For the FFT in the spaces and the transformed field domains of the spaces, the number of transformed points of 2048 and the distance increment of 1.27 cm (0.5 in.) were used. For the finite element model, the square plate elements with a length of each element of 5.08 cm (2 in.) were used. To model the infinite extent of the plate in the horizontal direction and to eliminate the effect of the boundary conditions, the stresses near the load, which were not affected by the size of the plate, were considered to compare with those obtained by the analytical method. The solutions of the finite element model were obtained using a finite element computer program, ABAQUS (ABAQUS, 1998). Note that the stresses at the top and bottom of the plate have the same magnitude with opposite signs.

Figure 3 shows the stresses at the plate bottom from the center of the load along the x direction for various values of the horizontal stiffness at the plate bottom. Fig. 3(a)

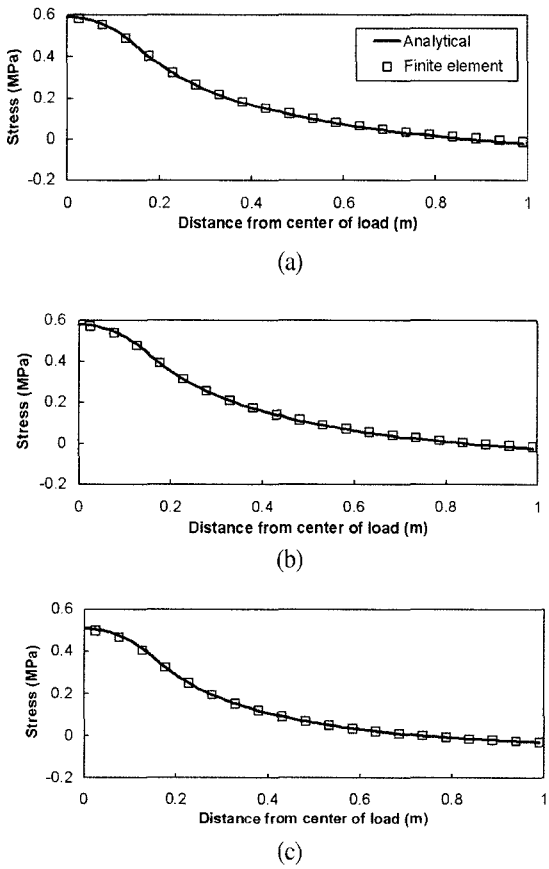

Fig. 3. Comparison between analytical and numerical analysis results: (a) $k_h = 0$ (b) $k_h = 408$ MN/m^3 (c) $k_h = 4{,}080$ MN/m^3

shows the stresses when there is no horizontal stiffness at the plate bottom. Excellent agreement can be observed between the analytical and finite element analysis results. When there is the horizontal resistance at the plate bottom, as shown in Fig. 3(b) (k_h = 408 MN/m^3 (1,500 pci)) and Fig. 3(c) (k_h = 4,080 MN/m^3 (15,000 pci)), the analysis results between the analytical and numerical methods also show very good agreement.

3.2. Horizontal resistance effects with vertical load

Figure 4 shows the effect of the horizontal resistance at the plate bottom on the maximum stress when the plate on a Winkler foundation is subjected to a vertical load. As the horizontal stiffness at the plate bottom increases, the maximum stress that occurs at the surface (compression in this study) and the bottom (tension) of the plate decreases. Because the horizontal stiffness at the plate bottom resists the bending of the plate, the stress becomes smaller as the horizontal stiffness increases.

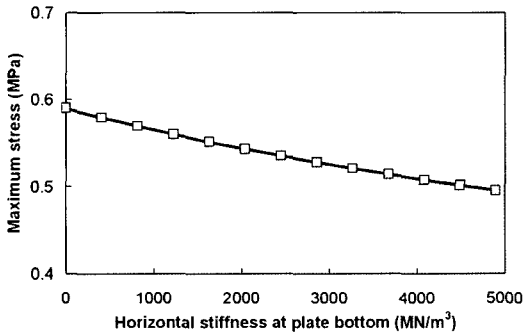

Fig. 4. Effect of horizontal resistance at plate bottom on maximum stress with vertical load

The differences in the maximum stresses of the plates on a Winkler foundation with and without the horizontal resistance at the plate bottom are investigated when the plate thickness, plate elastic modulus, and vertical stiffness of the foundation vary. The values of the plate thickness, plate elastic modulus, and vertical stiffness of the foundation considered in this study are within the practical ranges of those for concrete pavement systems (Kim et al., 2003). Figure 5(a) shows the percent ratio of the maximum stresses obtained with considering the horizontal resistance at the plate bottom to those obtained without considering the horizontal resistance when the thickness of the plate varies. The stress ratio smaller than 100% means that the stress obtained with considering the horizontal resistance is smaller than those obtained without considering it. As the plate thickness increases, the stress ratio decreases very slightly. This implies that the difference in the maximum stresses obtained with and without considering the horizontal resistance at the plate

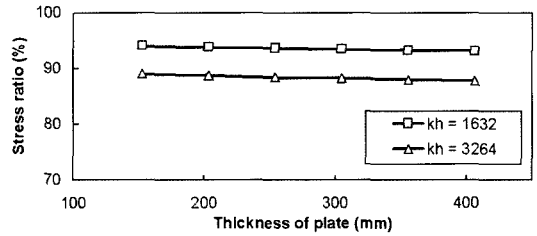

(a)

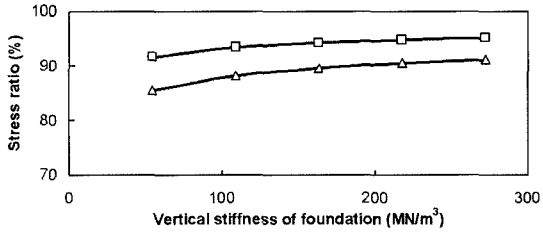

(b)

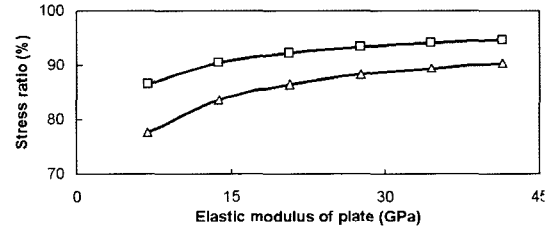

(c)

Fig. 5. Differences in stresses obtained with and without considering horizontal resistance when applying a vertical load for various values of: (a) plate thickness (b) vertical stiffness of foundation (c) plate elastic modulus (unit of k_h = MN/m^3)

bottom becomes slightly larger with increasing the plate thickness. Figure 5(b) shows the effect of the vertical stiffness of the foundation on the stress ratio. The stress ratio increases as the vertical stiffness of the foundation increases. This means that the difference in the maximum stresses obtained with and without considering the horizontal resistance at the plate bottom decreases with increasing the vertical stiffness of the foundation. The effect of the elastic modulus of the plate on the stress ratio is shown in Fig. 5(c). The stress ratio increases as the elastic modulus of the plate increases. Therefore, the effect of the horizontal resistance at the plate bottom on the maximum stress is significant when the thickness of the plate increases, the vertical stiffness of the foundation decreases, and the elastic modulus of the plate decreases. The maximum stresses obtained with considering the horizontal resistance at the plate bottom are always smaller than those obtained without considering it when the vertical load is applied.

4. Numerical modeling considering in-plane horizontal deformations

The formulations explained in the previous sections ignore in-plane horizontal deformations at the middle surface of the plate. More rigorous modeling of the plate on a Winkler foundation considering horizontal resistance at the plate bottom is to include horizontal axial deformations of the plate because the horizontal resistance at the plate bottom resists horizontal deformations of the plate as well as bending and curling of the plate. If the horizontal deformations are considered, the responses of the plate caused by horizontal axial loads such as a uniform temperature drop through the depth of the plate can also be obtained.

4.1. Finite element modeling

The in-plane horizontal deformations of the plate can be considered by adding two perpendicular horizontal degrees of freedom at each finite element node to the degrees of freedom in the plate bending element that has three degrees of freedom at each node as described previously. Then, the plate element has five degrees of freedom at each node and this element is often called a flat shell element.

If transverse shear deformations are neglected as in the thin plate theory, the straight lines that are initially normal to the middle surface of the plate remain straight and normal to the deflected middle surface. Accordingly, the effect of the horizontal resistance at the plate bottom can be considered with the shell elements by employing rigid beams as shown in Fig. 6(a). The degrees of freedom at

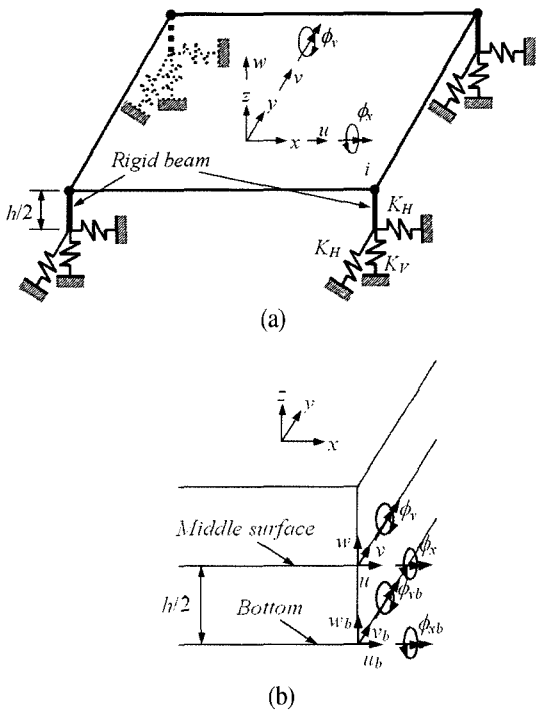

Fig. 6. Modeling considering in-plane deformations: (a) flat shell element with horizontal springs and rigid beams (b) degrees of freedom

node *i* and at the bottom of the plate (or bottom of the rigid beam) where the bottom resistance exists are shown in Fig. 6(b). Based on the assumptions in the thin plate theory, the vertical and rotational displacements at the middle surface and at the bottom of the plate are the same.

$$w = w_b, \quad \phi_x = \phi_{xb}, \quad \phi_y = \phi_{yb} \tag{17}$$

The horizontal displacements ub and vb at the bottom of the plate can be obtained using the displacements at the middle surface by

$$u_b = u - \frac{h}{2}\phi_y, \quad v_b = v + \frac{h}{2}\phi_x \tag{18}$$

where u and v are the displacements in the x and y directions at the middle surface, respectively, and $\emptyset_x$ and $\emptyset_y$ are the rotational displacements around the x and y axes, respectively. Then, the internal forces and moments created by the horizontal resistance at the plate bottom can be written as

$$F_x = K_H u_b = K_H u - \frac{h}{2}K_H\phi_y$$

$$F_y = K_H v_b = K_H v + \frac{h}{2}K_H\phi_x \tag{19}$$

$$M_x = K_H v_b \frac{h}{2} = \frac{h}{2}K_H v + \frac{h^2}{4}K_H\phi_x = \frac{h}{2}K_H v + K_R\phi_x$$

$$M_y = -K_H u_b \frac{h}{2} = -\frac{h}{2}K_H u + \frac{h^2}{4}K_H\phi_y = -\frac{h}{2}K_H u + K_R\phi_y$$

where F_x and F_y are the forces in the x and y directions, respectively, and M_x and M_y are the moments around the x and y axes, respectively. The horizontal stiffness K_H can be obtained multiplying the horizontal stiffness per unit area k_h by the effective area. Finally, the equilibrium equation at finite element node i (Fig. 6(a)) can be expressed as

$$\{F_i\} = \left(\begin{bmatrix} \text{Stiffness matrix of} \\ \text{flat shell} \\ \text{relative to node } i \end{bmatrix} + \begin{bmatrix} K_H & 0 & 0 & 0 & -\frac{h}{2}K_H & 0 & \cdots & 0 \\ 0 & K_H & 0 & \frac{h}{2}K_H & 0 & 0 & \cdots & 0 \\ 0 & 0 & K_V & 0 & 0 & 0 & \cdots & 0 \\ 0 & \frac{h}{2}K_H & 0 & K_R & 0 & 0 & \cdots & 0 \\ -\frac{h}{2}K_H & 0 & 0 & 0 & K_R & 0 & \cdots & 0 \end{bmatrix} \right) \begin{Bmatrix} u_i \\ v_i \\ w_i \\ \phi_{xi} \\ \phi_{yi} \\ \vdots \end{Bmatrix} \tag{20}$$

4.2. Comparison among different models

To verify the finite element model developed using the shell elements explained in the previous section, a more rigorous 3D finite element model was also developed using 3D solid elements. The size of a shell element was 7.62 cm (3 in.) by 7.62 cm (3 in.) and the size of a 3D solid element was 7.62 cm (3 in.) by 7.62 cm (3 in.) in the horizontal plane and 3.81 cm (1.5 in.) in the vertical direction. Therefore, the number of elements in the vertical direction for the 3D model was 8 to discretize a 12-inch thick plate. The horizontal stiffness at the plate bottom was assumed to be 1,632 MN/m³ (6,000 pci).

The stresses at the surface and bottom of the plate along the centerline in the x direction from three different models are shown in Fig. 7. The three different models include: (1) a model developed using the plate bending elements that have three degrees of freedom at each finite element node; (2) a model developed using the shell elements that have five degrees of freedom at each finite element node; and (3) a model developed using the 3D solid elements. As shown in Fig. 7, the results from the model developed using the shell elements and the 3D model are in excellent agreement. When the vertical load is applied, the models developed using the shell elements and the 3D solid elements yield slightly larger compressive stresses at the top of the plate and slightly smaller tensile stresses at the bottom of the plate compared with the results from the model developed using the plate bending elements. This happens because the horizontal resistance at the plate bottom resists the expansion of the bottom surface of the

plate caused by bending of the plate, and as a result, additional horizontal compressive stresses occur over the plate thickness. Since the model developed using the plate bending elements does not include the horizontal degrees of freedom, it cannot consider those additional stresses and the magnitudes of the stresses at the top and bottom of the plate are always the same with this model. In other words, the neutral surface where the stresses in the horizontal plane are zero is always the middle surface of the plate. On the other hand, in the models developed using the shell elements and the 3D solid elements, the neutral surface does not always remain at the middle surface and varies because of the additional horizontal stresses caused by the horizontal resistance at the plate bottom.

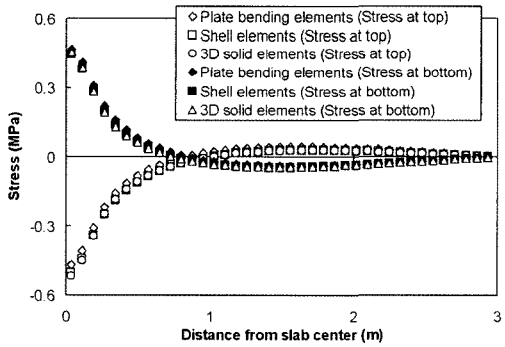

Fig. 7. Comparison between plates with and without considering in-plane deformations with vertical load

4.3. Horizontal resistance effects with vertical load

The effects of the horizontal resistance at the plate bottom on the stresses obtained with the model developed using the shell elements are very similar to the previous results obtained with the model developed using the plate bending elements, when the vertical load is applied. For instance, Fig. 8 shows the stress ratios between the plates on a Winkler foundation with and without considering the horizontal resistance, when the vertical load is applied. As investigated previously with the model developed using the plate bending elements, the stress ratio increases as the vertical stiffness of the foundation increases. The compressive stresses occurred at the top of the plate are close to those obtained without considering the horizontal resistance at the plate bottom (in other words, the stress ratios are close to 100%). However, the differences in the maximum tensile stresses occurred at the plate bottom obtained with and without considering the horizontal resistance are larger with the model developed using the shell elements.

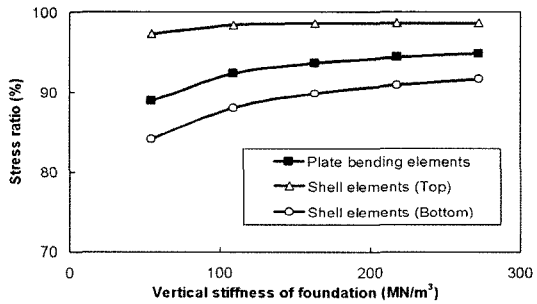

Fig. 8. Comparison of effects of horizontal resistance at plate bottom between plates with and without considering in-plane deformations with vertical load

5. Summary and conclusions

The behavior of the concrete slabs-on-grade considering the horizontal resistance at the slab bottom has been investigated employing the thin plate on a Winkler foundation when the system is subjected to a vertical load. Formulations have been developed analytically and numerically to include the effect of the horizontal resistance at the plate bottom. The sensitivity of the horizontal resistance to the stresses of the slab has been investigated with several material and geometric variables. The findings from this study are summarized as follows:

- By incorporating the internal horizontal forces occurred at the slab bottom caused by the horizontal resistance into the equilibrium equations, the governing

differential equation that include the horizontal resistance at the slab bottom can be obtained.

- The horizontal resistance effect can be considered in the finite element analysis with the plate bending elements and the flat shell elements without increasing the number of degrees of freedom.
- When the slab is subjected to a vertical load, the effect of the horizontal resistance at the slab bottom on the maximum stress becomes significant as the slab thickness increases and the elastic modulus of the slab and the vertical stiffness of the foundation decrease.
- If the in-plane horizontal deformations are considered, the location of the neutral surface changes from the middle surface of the slab due to the horizontal resistance at the slab bottom. As a result, the magnitudes of the stresses at the top and bottom of the slab are different; one increases and the other decreases.
- The analysis results obtained with the finite element model developed using the shell elements are basically the same as those obtained with the model developed using the 3D solid elements when the horizontal resistance at the slab bottom is considered. Since the model consisting of the shell elements needs much smaller computation time and memory compared with the 3D analysis, it is very useful for practical purposes.

Acknowledgment

This research was supported by the Kyung Hee University Research Fund in 2003. The financial support of Kyung Hee University is sincerely appreciated.

References

1. ABAQUS. (1998). "*User's manual version 5.8.*" Hibbit, Karlsson & Sorensen, Inc.
2. Huang, M. H. and Thambiratnam, D. P. (2001). "Deflection response of plate on Winkler foundation to moving accelerated loads." *Engineering Structures*, Vol. 23, Issue 9, pp. 1134-1141.
3. Huang, Y. H. (1993). "Pavement analysis and design." Prentice Hall, New Jersey.
4. Kim, S. M., Nam, J. H., and McCullough, B. F. (2003). "Sensitivity of design variables to continuously reinforced concrete pavement behavior." *Proceedings of the 82nd Annual Meeting of Transportation Research Board,* Washington, D.C. (CD-ROM).
5. Kim, S. M. and Roesset, J. M. (1997). "Dynamic response of pavement systems to moving loads." *Geotechnical Engineering Report GR97-4,* Geotechnical Engineering Center, The University of Texas at Austin.
6. Kim, S. M. and Roesset, J. M. (1998). "Moving loads on a plate on elastic foundation." *ASCE Journal of Engineering Mechanics*, Vol. 124, No. 9, pp. 1010-1016.
7. Kim, S. M., Won, M. C., and McCullough, B. F. (2002). "Dynamic stress response of concrete pavements to moving tandem-axle loads." *Transportation Research Record Journal of the Transportation Research Board*, No. 1809, pp. 32-41.
8. Kim, S. M., Won, M. C., and McCullough, B. F. (2000). "Three-dimensional analysis of continuously reinforced concrete pavements." *Transportation Research Record Journal of the Transportation Research Board*, No. 1730, pp. 43-52.
9. Liu, C., McCullough, B. F., and Oey, H. S. (2000). "Response of rigid pavements due to vehicle-road interaction." *ASCE Journal of Transportation Engineering,* Vol. 126, No. 3, pp. 237-42.
10. Tabatabaie, A. M. and Barenberg, E. J. (1980). "Structural analysis of concrete pavement systems." *ASCE Transportation Engineering Journal*, Vol. 106, No. 5, pp. 493-506.
11. Westergaard, H. M. (1925). "Stresses in concrete pavements computed by theoretical analysis." *Public Roads,* Vol. 7, pp. 25-35.

〈접수 : 2005. 8. 30〉